Visual Abstract

Mesoscale investigation of mass concrete temperature control systems and their consequences on concrete mechanical behaviour

A. Taibi, T.T Chimoto, F.K Maradzika, M. Matallah
RISAM, University Abou Bekr Belkaid Tlemcen, Algeria
taibi.abdelsemi@gmail.com, https://orcid.org/0000-0003-2301-3472
tawandattch@gmail.com, faraikelvinmaradzika@gmail.com
mohammed.matallah@gmail.com, https://orcid.org/0000-0002-9679-9878

ABSTRACT. This study investigates the impact of aggregate and pipe cooling systems on concrete behaviour at a mesoscale level. Firstly, a Chemo-Thermo-Mechanical model is developed to investigate the initial stress state of early age hydration concrete followed by a mechanical analysis of the consequences brought by this initial state. Pipe and aggregate cooled concrete samples have been subjected to tensile and cyclic loadings. The results have been discussed in terms of damage and crack openings. It has been concluded that early age hydration modifies the initial conditions of any concrete structures. Regarding the cyclic behaviour, initial state due to the hydration process leads to permanent displacements corresponding to damage and cracking. The cooling methods improve the mechanical behaviour of concrete.

KEYWORDS. Early age behaviour; Pipe cooling; Aggregate cooling; Mesoscale modeling.

OPEN ACCESS

Citation: Taibi, A., Chimoto, T. T., Maradzika, F. K., Matallah, M., Mesoscale investigation of mass concrete temperature control systems and their consequences on concrete mechanical behaviour, Frattura ed Integrità Strutturale, 60 (2022) 416-437.

Received: 22.01.2022
Accepted: 18.03.2022
Online first: 20.03.2022
Published: 01.04.2022

INTRODUCTION

Advances in both technology and the never-ending needs of the modern society has ushered in the construction of mega-structures which accommodate an enormous space capacity in a single structure such as large footings, concrete gravity dams, nuclear reactors and powerhouses, large-area concrete slabs [1]. When a vast bulk of fresh concrete is cast, questions on the effects of the hydration reaction of cement with water which brings about initial stress conditions in concrete arise. Emission of considerable hydration heat from the exothermic reaction and the relatively lower conductivity coupled with the large size of the concrete material lead to the manifestation of adiabatic conditions in a mass concrete [2]. The heat at the core of the mass concrete prompts the need for internal cooling or use of low-heat-producing materials to be used [3]. Studies contend that plain cement paste cured above 50°C has large pores and increased permeability which brings about corrosion of the embedded reinforcing steel and inadvertently impair the durability, integrity of the concrete structure in the long-term [4]. Moreover, it's derived that temperature at concrete surfaces are relatively lower than those at the core of the concrete mass due to surface heat loss to external ambient cooling. This creates a temperature difference which may lead to tensile stresses higher than the tensile strength of concrete, affecting its durability and serviceability due to cracking [5]. The genesis of high-performance concretes and their increasing relevance in the built environment has given rise to concerns in traditionally thin structural members with

respect to early age concrete cracking [6]. Also, of concern to contractors, designers and researchers are the negative effects on the aesthetics of the structure [7]. To enhance the integrity of mass concrete, various temperature control measures exist. If administered, they prevent cracking by regulating the initial stresses provoked by the hydration process of cement in concrete [8]. Various techniques are available in the literature to constrain the thermal gradient in concrete, such as the precooling methods of an ice-water mixture or liquid nitrogen to lower the temperature of fresh concrete [9] or concrete mixed with MgO to delay the concrete volume expansion [10], the post cooling methods including but not limited to, use of cooling pipes embedded in concrete for heat removal [11], surface curing and so on. Curing period and curing temperature influence both the early and later age strengths [12]. Over the past two decades, relevant experimental programs and numerical models were developed to predict the early age behaviour of concrete and the effect of cooling methods on the mechanical behaviour [13–16]. Largely, this paper explores aggregates and pipes cooling methods. For the latter, the principle is to lay thin pipes in the structure. As concrete casting kick-starts, cold water is pumped into these pipes to limit the temperature rise inside the concrete during the hydration. During the cooling process, the water gets warmed up by absorbing the heat from the hydration of concrete. However, use of piped water cooling in mass concrete can trigger adverse effects as there's a potential creation of an extreme temperature gradient within the concrete around the cooling pipes, presenting significant thermal stresses which are enough for cracking to yield [17]. According to [18], in massive structures, a 6℃ lowering of the placing temperature below the average air temperature will result in a 3℃ decrease of the maximum temperature reached by the concrete. These findings surmise that the lower the temperature of the concrete when it passes from a plastic condition to an elastic state upon hardening, the less will be the tendency toward cracking. Cognizant of the fact that aggregates occupy the greatest part of a concrete mixture, a change in the temperature of the aggregates will translate to the greatest change in the temperature of the concrete. It's proffered that the amount of cement in lean mass concrete mixtures is relatively small; cooling under a control program is inutile. A plethora of methods for aggregate cooling exist ranging from cold weather aggregate processing to chilled water spraying. However, depending on the context, the use of other methods could achieve better results when dealing with the insanely high temperature in mass concrete. Costs have to be factored in as well, for methods such as pipes cooling surge the construction costs. It then would be of great service to use surface insulation in place of pipes cooling for it is cheaper and easy to implement, unfortunately it slows down the construction process as temperatures will be stabilizing. Although many attempts have been made to model the influence of early age state on the mechanical behaviour of concrete, the effect of aggregate and the pipe cooling systems on concrete behaviour at early age was rarely investigated at a mesoscopic scale. A full description of aggregate/pipe based cooling systems needs a mesoscale approach where concrete constituents are explicitly represented. The meso-scale permits an explicit representation of the concrete constituents where concrete is considered as a biphasic material. The mortar and the aggregate phases are described by their own characteristic behavior.
Herein, a mesoscale investigation of the initial stress conditions of a concrete undergoing early age hydration is undertaken and the subsequent consequences of these initial stresses on the mechanical behaviour of concrete are analyzed. A study on the mass concrete hydration temperature control systems is as well undertaken with the resultant impact on the mechanical behaviour of concrete. These studies are conducted by means of 2D mesoscopic chemo-thermo-mechanical model implemented in the free FE software Cast3M. Developed by the French Atomic Energy Commission (CEA), Cast3M is a software based on the finite element method for the mechanical and heat transfer analysis of linear and non-linear problems in structures and fluids.
Static-monotonic and cyclic loadings are considered to study the mechanical analysis of the consequences brought by the hydration initial state. A damage-plasticity based model is employed to describe the softening behaviour of concrete. The theory of continuum damage mechanics (CDM) coupled with plasticity is considered as an attractive way to deal with concrete degradation [19–22]. The concrete is considered as a two-phase material, composed of aggregate and the concrete paste matrix. All aggregates whose diameter is less than 2.5mm are considered as part of the matrix. For aggregate cooling investigation, the initial temperature of the aggregates is considered different from that of the matrix and it is also considered that only the matrix undergoes hydration. A theoretical aggregate geometry is adopted; aggregates are considered as circular in shape. The Chemo-Thermo-Mechanical model developed is firstly presented. Subsequently, the results of the numerical investigation are discussed.

CHEMO-THERMO-MECHANICAL MODEL

The hydration of cement paste is a thermo-activated process. This process may be expressed with an Arrhenius type law. The evolution of hydration is achieved by the use of a chemical affinity [23]:

[1] $$\dot{\xi} = \tilde{A}(\xi).\exp(\frac{E_a}{RT}) \quad (1)$$

where E_a is the activation energy $\left[J.mol^{-1}\right]$,R is the ideal gas constant, T is the temperature $\left[K\right]$, ξ is the hydration degree and $\tilde{A}(\xi)$ is the chemical affinity $\left[S^{-1}\right]$given by

$$\tilde{A}(\xi) = a + b\xi + c\xi^2 + d\xi^3 + e\xi^4 + f\xi^5 + g\xi^6 \quad (2)$$

where a, b, c, d, e, f and g are constant material parameters which could be identified from a semi-adiabatic test. The energy balance equation, which includes the heat release due to hydration reaction is solved to obtain the temperature evolution [24]:

$$C\dot{T} = \nabla(k\nabla T) + L\dot{\xi} \quad (3)$$

In which L is the latent hydration heat $\left[Jm^{-3}\right]$,k is the thermal conductivity $\left[Wm^{-1}K^{-1}\right]$ and C is the volumetric heat capacity $\left[Jm^{-3}K^{-1}\right]$, which is assumed constant. The boundary conditions are assumed to be of convective type. The convective heat flux $\phi\left[Wm^{-2}\right]$ reads:

$$\phi = h(T_s - T_{ext}) \quad (4)$$

where h is the exchange coefficient including convection (after linearization)$\left[Wm^{-2}K^{-1}\right]$, T_s is the temperature on the surface $\left[K\right]$ and T_{ext} is the ambient temperature $\left[K\right]$ [24].
The thermal strain is related to the temperature variation, due to the release of heat by hydration, and the coefficient of thermal expansion α (considered as constant):

$$\dot{\varepsilon}_{th} = \alpha\dot{T}I \quad (5)$$

As concrete hardens, autogenous shrinkage develops. The autogenous shrinkage is related to the evolution of hydration. Experimental results show that autogenous shrinkage evolution is linear with respect to the hydration degree. The autogenous shrinkage ε_{au} could be described by [23] :

$$\dot{\varepsilon}_{au} = -k\dot{\xi}I \text{ for } \xi > \xi_0 \quad (6)$$

The evolution of the mechanical parameters (Young's modulus, Poisson's ratio, tensile strength …) with respect to hydration process will be discussed after presenting the mechanical damage model.

DAMAGE PLASTICITY MODEL FOR THE NON-LINEAR BEHAVIOUR OF CONCRETE

The non-linear mechanical behaviour of concrete is described by a damage model. The model used has been developed by [19]. The effective stress in the damaged material is related to the macroscopic stress. The relationship between stress and strain tensors is given by:

$$\sigma_{ij} = C_{ijkl}^{damaged} \varepsilon_{kl} \tag{7}$$

where $C_{ijkl}^{damaged}$ is the stiffness of the damaged material. The effective stress $\tilde{\sigma}$ is given by :

$$\tilde{\sigma}_{ij} = C_{ijkl}^{0} (C_{ijkl}^{damaged})_{klmn}^{-1} . \sigma_{mn} \tag{8}$$

C_{ijkl}^{0} is the initial stiffness tensor. For the isotropic version of the model (where damage is described by a scalar parameter), the relation between total stress σ_{ij} and effective stress $\tilde{\sigma}_{ij}$ is given by the expression below [25]:

$$\sigma_{ij} = (1-d)\tilde{\sigma}_{ij} \tag{9}$$

where d is the damage variable. Physically, the variable d is defined as the ratio between micro crack surface and that of the total section material. The evolution law of the scalar damage variable is given through the normality rule using the following loading function:

$$f = \varepsilon - \varepsilon_{d0} - \zeta \tag{10}$$

where ξ_{d0} is the damage threshold. ζ is a hardening/softening variable. After integration, the evolution law is written as [19]:

$$d = 1 - \frac{\varepsilon_{d0}}{\varepsilon} \exp(B(\varepsilon_{d0} - \varepsilon)) \tag{11}$$

B is a parameter which commands the slope of the softening curve defined by the exponential expression. In its original version, the model couples damage and plasticity. In the present work, plasticity is not considered.

CRACK OPENING ESTIMATION

FEM-based continuous approaches are based on an indirect representation of cracking by inelastic strains smeared uniformly across the width of the localized failure band. The strain-softening behavior leads to ill-posedness of the boundary value problem and spurious mesh sensitivity in finite element computations. To capture the non locality during the cracking process, various regularisation methods have been proposed to deal with mesh sensitivity, including non-local or gradient continua, Cosserat continua etc. [26]. When dealing with Diffuse Interface Modeling approaches, Pascuzzo et al [27] show that the use of zero-thickness interface elements, whose strength and toughness properties are spatially randomized, presents a reliable numerical tool to avoid the well-known mesh dependency issues. Another simple remedy for the spurious mesh sensitivity caused by the strain softening is to adopt the crack band model based on the fracture energy regularization [28]. Indeed, the crack band model, in which the crack is smeared over the finite element of a width equal to the crack band width, has been successfully used to deal with concrete fracture process. In this investigation, the practical method to estimate crack opening from a finite element computation based on damage and/or plastic models developed by Matallah et al [25] is used. This method, based on the fracture energy regularization, is proposed in the Finite Element code Cast3M (OUVFISS Procedure). The basic idea is that if the finite element size is modified, then the material parameters that control the damage-cracking strain must be adjusted in such a way that the energy dissipated by large and small elements per unit length and width of the crack band would be identical. This method is applicable to all continuous damage-plasticity based models. The softening behaviour is governed by the fracture energy parameter. Under tensile loading G_f is given by:

$$G_f = h\int_0^\infty E(1-d)\varepsilon d\varepsilon = h\int_0^\infty E\frac{\varepsilon_{d0}}{\varepsilon}\exp(B(\varepsilon_{d0}-\varepsilon\ ))\varepsilon d\varepsilon = h(\frac{{\varepsilon_{d0}}^2}{2}+\frac{\varepsilon_{d0}}{B}) \tag{12}$$

After the finite element computation using the nonlinear damage/plasticity model, the stress tensor is calculated by Eq. (13):

$$\sigma_{ij}^e = C_{ijkl}^0\varepsilon_{kl} \tag{13}$$

The total deformation in the concrete ε_{ij} is decomposed into two parts, namely :(i) an elastic part ε_{ij}^e and (ii) a cracking part represented by the unitary crack opening deformation tensor (Unitary Crack Opening) ε_{ij}^{uco}

$$\varepsilon_{ij} = \varepsilon_{ij}^e + \varepsilon_{ij}^{uco} \tag{14}$$

By multiplying Eq. (14) by the undamaged elastic stiffness tensor C_{ijkl}^0 , we obtain:

$$\sigma_{ij}^e = C_{ijkl}^0\varepsilon_{kl} = C_{ijkl}^0\varepsilon_{kl}^e + C_{ijkl}^0\varepsilon_{kl}^{uco} = \sigma_{ij}^s + \sigma_{ij}^{in} \tag{15}$$

So, the tensor of the crack opening strain is given by:

$$\varepsilon_{ij}^{uco} = (C_{ijkl}^0)^{-1}\sigma_{ij}^{in} \tag{16}$$

The inelastic stress tensor is therefore given by:

$$\sigma_{ij}^{in} = \sigma_{ij}^e - \sigma_{ij}^s \tag{17}$$

Eq.(16) gives the Unitary Crack Opening strain tensor. The normal crack opening displacement value is given by:

$$\delta_n = n_i\delta_{ij}n_j = n_i h\varepsilon_{ij}^{uco}n_j \tag{18}$$

$\vec{n}$: the unit vector normal to the crack, δ_n : the normal displacement of the crack opening. The method has been validated under different arbitrary loadings and complex boundary conditions [29–31].

EVOLUTION OF THE MECHANICAL PARAMETERS WITH RESPECT TO THE HYDRATION DEGREE

During the hydration process, the mechanical properties are evolving:

- *Young's Modulus* for the Young's modulus, the following equation is adopted

$$E(\xi) = E_\infty\overline{\xi}^\beta \tag{19}$$

With $\overline{\xi} = \left\langle\frac{\xi-\xi_0}{\xi_\infty-\xi_0}\right\rangle_+$ in which ξ_0 is the mechanical percolation threshold. It is kept constant and equal to 0.1. ξ_∞ is the final hydration degree. E_∞ is the final Young's modulus, β is a constant equal to 0.62. $\langle\ \rangle_+$ refers to the positive part operator.

- *Poisson ratio:*

The Poisson ratio is relatively stable for concrete. Neville [32] recommends a value equal to 0.2 for most concrete mixes. However, De Schutter [33] suggests an evolution depending on the hydration degree as follows

$$\upsilon = 0.18\sin\frac{\pi\xi}{2} + 0.5\exp(-10\xi) \tag{20}$$

- *Tensile strength*

$$f_t(\xi) = f_{t\infty}\overline{\xi}^{\gamma} \tag{21}$$

where $f_{t\infty}$ is the final tensile strength, γ is taken as equal to 0.46.

The evolution of the tensile strain threshold ε_{d0} is computed from the evolution of f_t and E.

$$\varepsilon_{d0}(\xi) = \frac{f_t(\xi)}{E(\xi)} = \frac{f_{t\infty}}{E_{\infty}}\overline{\xi}^{\gamma-\beta} = \varepsilon_{d0\infty}\overline{\xi}^{\gamma-\beta} \tag{22}$$

- *Fracture energy*

The fracture energy is represented by the stress-crack opening displacement curve under tension. Using the damage formulation exposed above, the fracture energy is given by:

$$G_f = h\int_0^{\infty} E(1-d)\varepsilon d\varepsilon = h\int_0^{\infty} E\frac{\varepsilon_{d0}}{\varepsilon}\exp(B(\varepsilon_{d0}-\varepsilon))\varepsilon d\varepsilon = Eh(\frac{{\varepsilon_{d0}}^2}{2} + \frac{\varepsilon_{d0}}{B}) \tag{23}$$

The term $(\xi_{d0}^2/2)$ could be neglected. The length scale which is introduced into the model is the finite element size h. For the numerical simulation, the damage parameter B is function of h of and controls the slope of the strain softening curve [34]

$$B = h\frac{f_t}{G_f} \tag{24}$$

So, using the evolution equation of f_t and G_f, we propose the following evolution of B as:

$$B(\xi) = B_{\infty}\overline{\xi}^{\gamma-\alpha} \tag{25}$$

with $B_{\infty} = h\dfrac{f_{t\infty}}{G_{f\infty}(1-\mathrm{H})}$, and $\alpha = 0.8$.

VALIDATION OF THE CTM MODEL

In this section, we evaluate the reliability of the CTM model presented above. The validation is done by comparing temperature results of a numerical simulation at 3D scale with experimental and numerical results given by Sofi el al [35]. The development of temperature in massive structures is influenced by various factors such as the initial temperature (which depends on the cooling process), external conditions, cement type, formwork type, etc. In [35], a block of concrete was made and cured under laboratory conditions to monitor the temperature development in the concrete. The concrete block was cured under laboratory conditions with a constant temperature of 20 ± 3 C°, RH = 70%. The concrete temperature development was monitored over time using three sensors at different depths. Both

numerical and experimental results obtained in [35] are used to validate the CTM model. The concrete block dimensions and the FE mesh 3D are shown in Fig. 1. The channels are located at different depths of the block concrete in order to capture the evolution of temperature in the block. Thus, the sensors C1, C2 and C3 were respectively placed at 100 mm, 150 mm and 200 mm. The ambient temperature evolution is presented in Fig. 2. The thermal properties of concrete and the boundary conditions are summarized in Tab. 1. Fig. 3 shows the comparison between the numerical results obtained by the CTM model developed and the results from [35] at the level of sensor 3. Results show good agreement with deviations that never overcome 2°C.

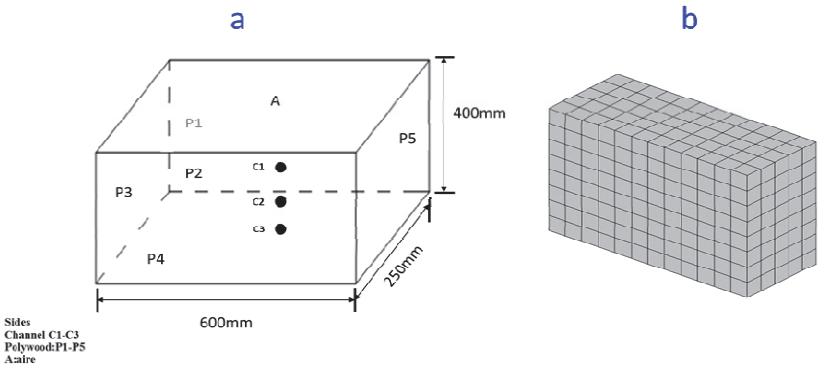

Figure 1: Concrete block: (a) dimensions and location the thermocouple; (b) 3D FE mesh.

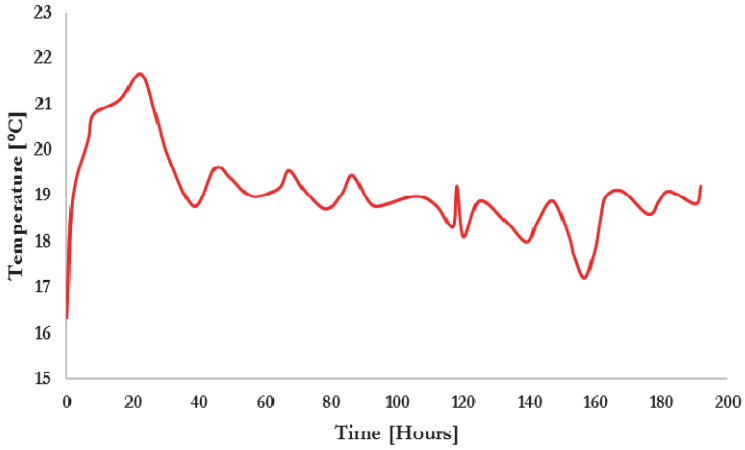

Figure 2: Ambient recorded temperature.

Parameter	Value
Concrete thermal conductivity	2(W/m K)
Concrete volumetric heat specific capacity	$4600\,(KJ\,/\,m^3K^{-1})$
Convection-radiation coefficient between concrete and air	$7.5\,(Wm^{-2}K^{-1})$
Equivalent convection-radiation coefficient between concrete and Framework	$6\,(Wm^{-2}K^{-1})$
Arrhenius constant Ea/R	4000 (°K)
Latent hydration heat	$137000\ (KJ\,/\,m^3)$
a	16.62
b	50.81
c	192.21
d	-1173.77
e	602.27
f	1624.42
g	-1367.28

Table 1: Thermal properties and parameters of the CTM model.

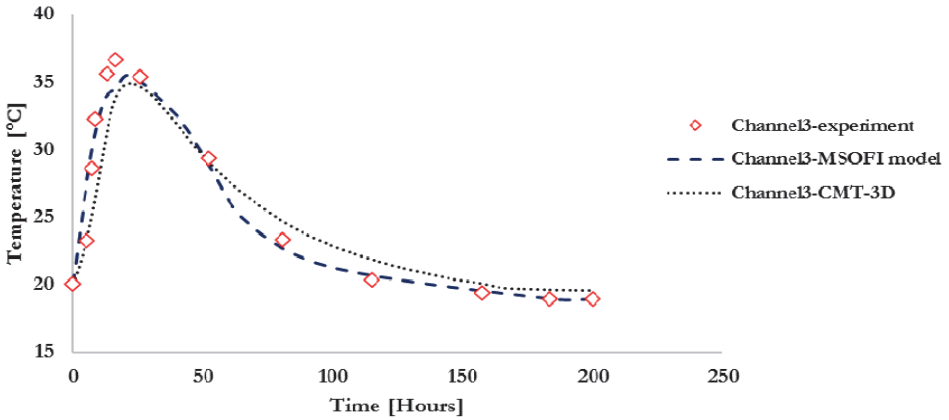

Figure 3: Concrete temperature: CTM Vs results from [35].

MESOSCOPIC MODELING OF EARLY AGE BEHAVIOUR

As stated, this study will be carried out at a mesoscale level, i.e. the concrete will be considered a heterogeneous material with aggregates and mortar matrix. The meso-scale permits an explicit representation of concrete constituents [29]; [30]; [36]. Only the mortar matrix undergoes early age hydration. The fracture behaviours of the aggregates and of the mortar matrix follow the isotropic damage model with damage parameters corresponding to each component. The Interfacial Transition Zone (ITZ) is not considered. Due to mechanical parameters contrasts (elastic and fracture parameters), stress concentrations occur at the aggregate-matrix interface and lead to damage creation. The impact of the ITZ has been extensively discussed by Grondin and Matallah in [37]. A list of all the input mechanical parameters is presented in Tab. 2. As stated before, these parameters are evolving with hydration. Tab. 2 gives the values of the mechanical parameters at final hydration.

	$E_{\infty}(GPa)$	ν_{∞}	$F_{t\infty}(MPa)$	$G_{f\infty}(N/m)$
Mortar	15	0.2	3	20
Coarse aggregate	60	0.2	6	60

Table 2: Model parameters.

Diameter (mm)	Volumetric (%)
21	4
20	6
16	6
14.5	8
12	8
10.5	6
7	4
5	4

Table 3: Volume fraction of each granular class.

The finite element problem is solved using the classical procedure for nonlinear problems that is implemented in the Cast3M code [38]. The numerical concrete has its aggregates randomly distributed in the concrete specimen to form the granular skeleton and the cement paste (matrix) fills the space between the aggregates. In the model, the matrix depends entirely on the spatial distribution of the aggregates. The digital concrete specimen is represented in 2D form. Tab. 3 shows the granular class composition used. The shape of the aggregates used in this simulation is circular. Although this is

not the case in practicality, the impact of the geometry of the aggregate in the model is minimal to the study we are going to be focusing on. Fig. 2 shows the (10×10) cm² and (20×20) cm² sample meshes.

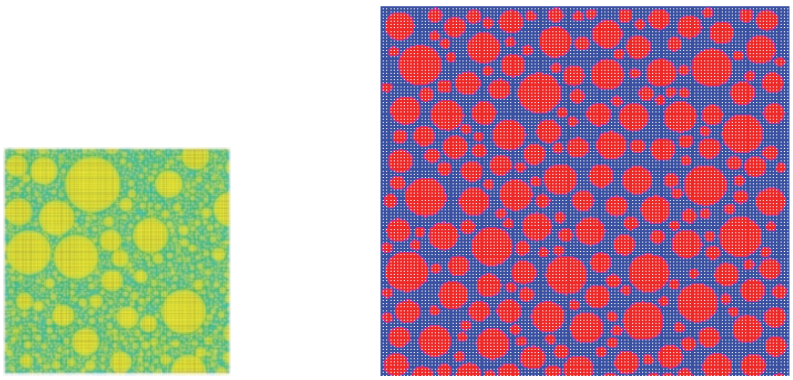

(10*10) cm² (20*20) cm²

Figure 4: Mesoscopic mesh for the two samples.

The behaviours of the two samples are firstly simulated under hydration to investigate the initial state after hydration. The size of mesh is related to the smallest considered aggregate. In this investigation, quadrangle elements (QUA4) of 0.4mm size were used to model aggregates and mortar, whereas a number of 536 segment elements (2-node line) were used to mesh the cooling pipes. Fig. 5 shows an example of the pipe cooling meshing. Parameters for pipe cooling listed in Tab. 4 were adopted from [39]. For aggregate cooling system, Tab. 5 shows the initial temperatures for aggregate cooling. Tab. 6 gives the other parameters used in the simulations.

Characteristics of the cooling pipe system	Values
The coefficient of convective heat transfer on the pipe loop, W / (m² °C)	282
Speed, m/s	0.5
Water temperatures in the pipes, K	293
The density of water, kg / m³	1000
Specific heat capacity, kJ/ (kg °C)	1.12
Thermal conductivity, w / (m °C)	0.64
Pipe radius, m	0.003
The duration of cooling	172hrs
Ambient temperature, K	293

Table 4: Model parameters for the cooling pipes.

Type	Initial Temperature (K)
Aggregates	283
Cement paste	293

Table 5: Initial temperatures for aggregate cooling method.

Characteristics of the cooling pipe system	Values	Units
Volumetric mass	2500	kg/m³
Volumetric heat capacity	2400	kJ / (m³ °C)
Thermal conductivity of concrete	2.6	W / (m. °K)
Activation energy	45729.75	J / mol
Gas constant	8.3145	J / (K. mol)
Convection coefficient	12.5	W / (K. m²)
Latent heat of hydration	117840	kJ. m³
Chemical affinity	1.2	s^{-1}
Thermal coefficient	7.5	µm / (m. °C)
Final endogenous shrinkage	40	µm / m
A	64.417	
B	18042	
C	-94620	
D	215819	
E	-280339	
F	208172	
G	-67901	
Ambient room temperature	293	K

Table 6: Other parametric values used in the simulations.

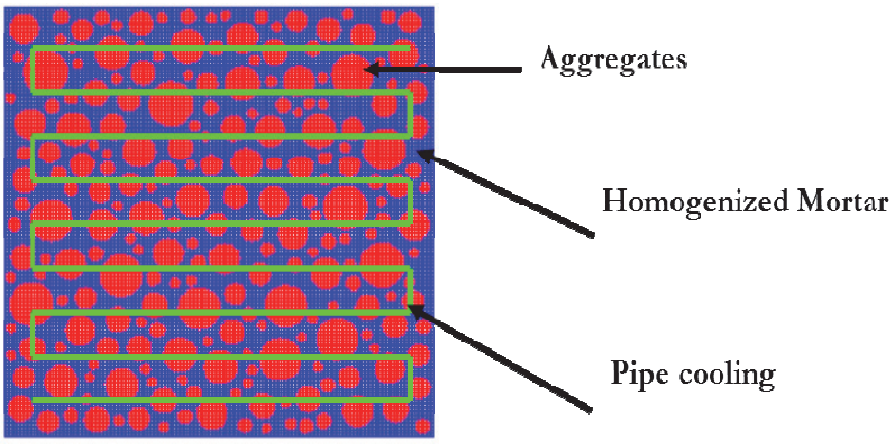

Figure 5: Pipe cooling mesh.

After hydration, the concrete samples are subjected to uni-axial tensile and cyclic loading. The numerical simulations are driven under 2D plane stress condition. The samples are isostatically restrained. Before the mechanical loading, initial states are simulated with and without cooling. For tensile and cyclic loading, computations are driven under displacements control Δ (Fig. 6).

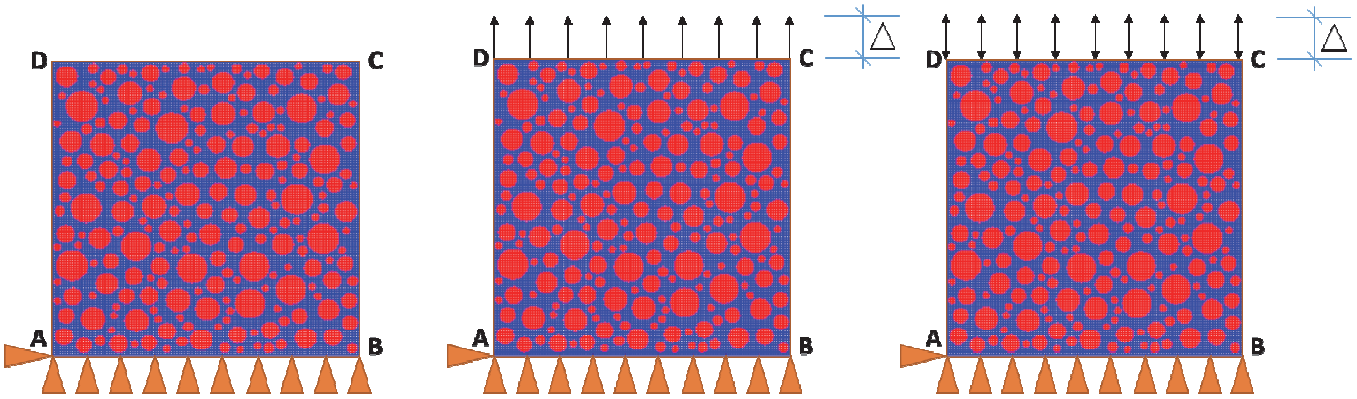

Figure 6: Pipe cooling mesh. Boundary conditions. (a) Early age only, (b) Early Age + Traction, (c) Early Age + Cyclic loading.

NUMERICAL SIMULATION OF EARLY AGE BEHAVIOUR

Below are findings from the numerical simulation of early age state of the concrete samples followed by a mechanical analysis of the consequences brought by this initial state under tensile and cyclic loadings. Two concrete specimens of different dimensions (10×10) cm² and, (20×20) cm² were simulated with early age to analyse the effects of geometry or dimensions on the maximum hydration temperature in concrete. Fig. 7 shows the temperature evolution of the two samples.

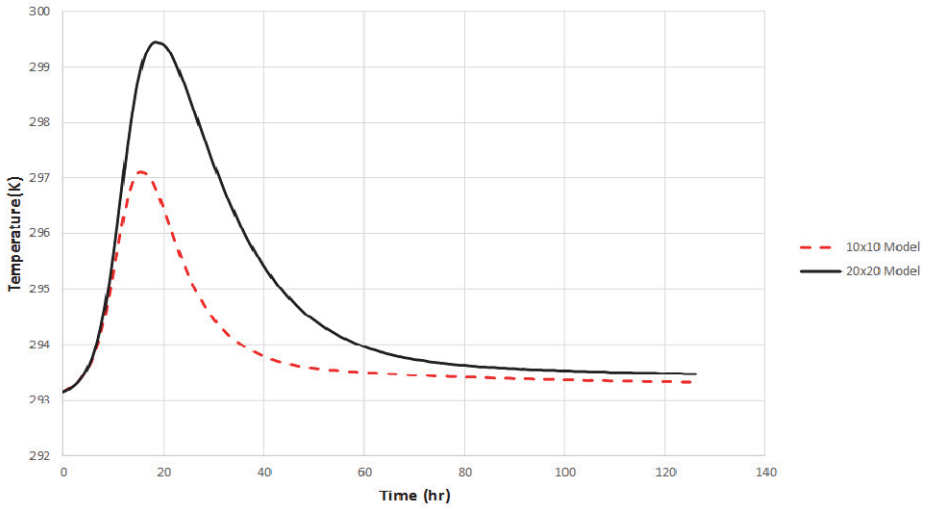

Figure 7: Hydration temperature evolution of a (10×10) cm² model and a (20×20) cm² model.

As observed from Fig. 7, a lower peak and a favourable thermal evolution in the (10×10) cm² sample is witnessed as compared to the (20×20) cm² one. These observations further demonstrate the vulnerability of massive structures with respect to early age hydration. The (20×20) cm² sample will be chosen for the following simulations. Obviously, larger dimensions could be used; however, mesoscale computations are very time consuming.

EFFECT OF EARLY AGE ON MECHANICAL BEHAVIOUR OF CONCRETE

Fig. 8 shows stress, damage and crack openings for concrete with early age hydration. Obviously, concrete without considering early age hydration does not exhibit any stresses, damage or crack openings.

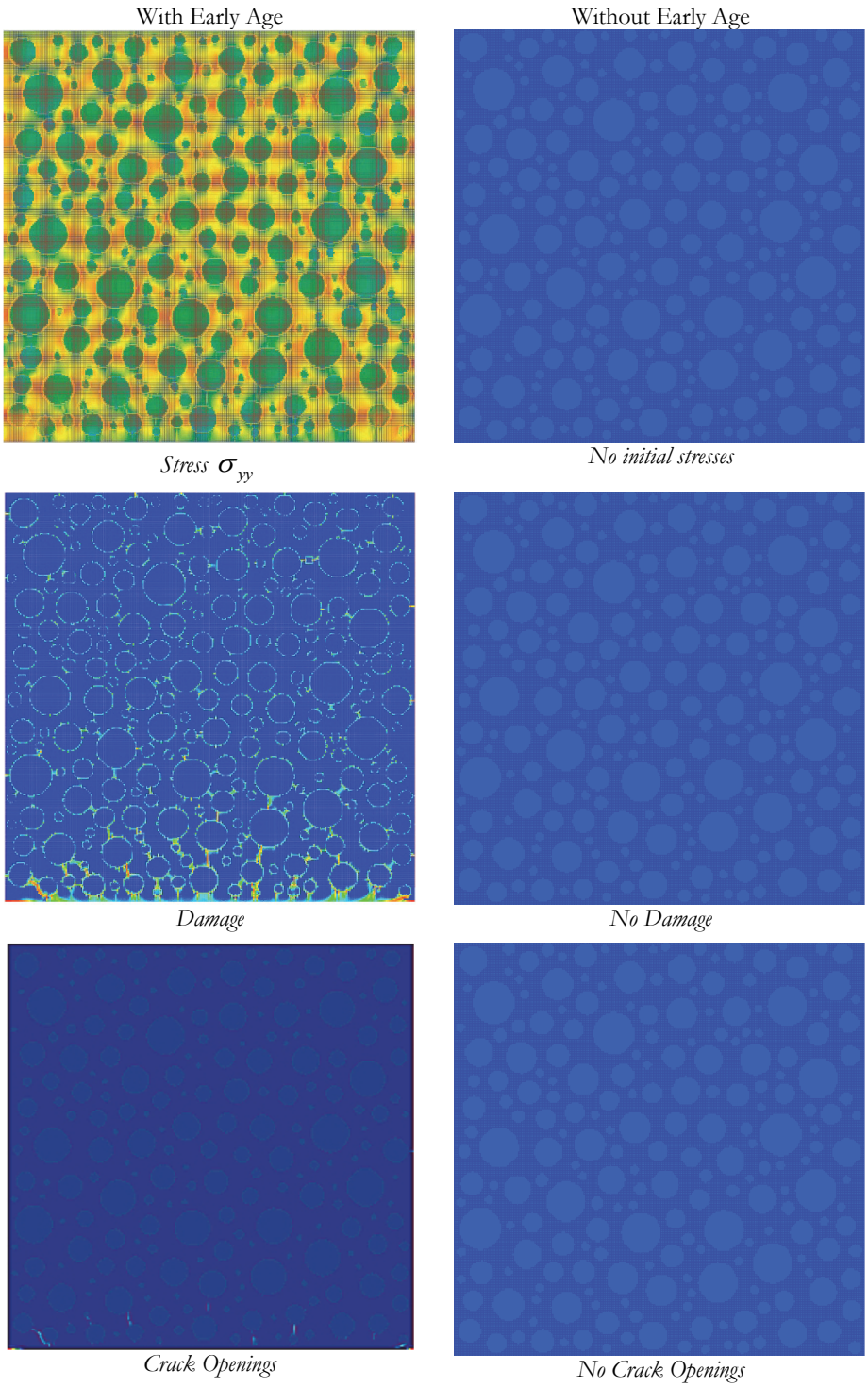

Figure 8: Stress, damage and crack openings due to early age hydration without cooling.

GLOBAL AND LOCAL BEHAVIOURS UNDER TENSILE LOADING

To study the mechanical analysis of the consequences brought by the hydration initial state, the behaviour of the (20×20) cm² sample is simulated under tensile loading. Fig. 9 shows stress-displacement evolution of early age concrete and concrete without early age under traction. Concrete with initial state shows a *premature* non-linear behaviour due to the existence of initial stresses (The elastic phase in not linear). Regarding the peak strength, the two

simulations show quite similar results. However, local behaviour shows a noticeable difference. Fig. 10 shows damage and crack opening evolution of early age concrete and concrete without early age under traction loading. Crack openings have been estimated using the post-processing method exposed above (Matallah and al [25]). A more significant damage density is witnessed on early age concrete. Regarding crack opening values, concrete with initial early age state shows higher crack openings. Cracks propagate in the matrix perpendicular to the loading directions.

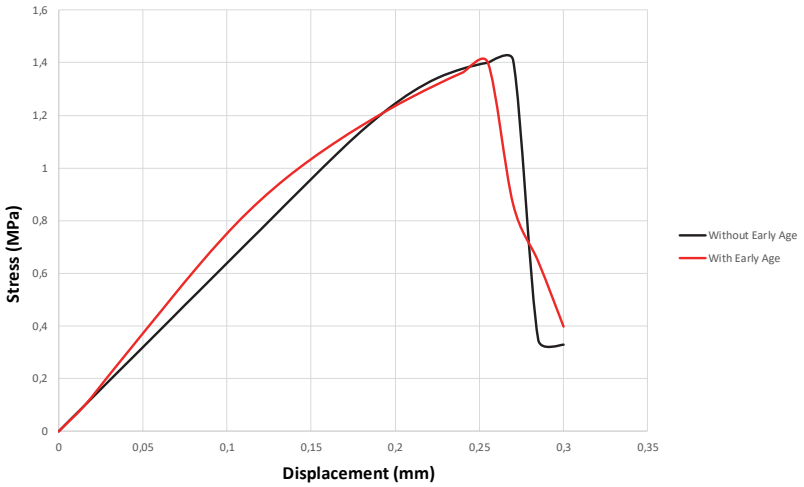

Figure 9: Global mechanical behaviour of early age concrete under tensile loading.

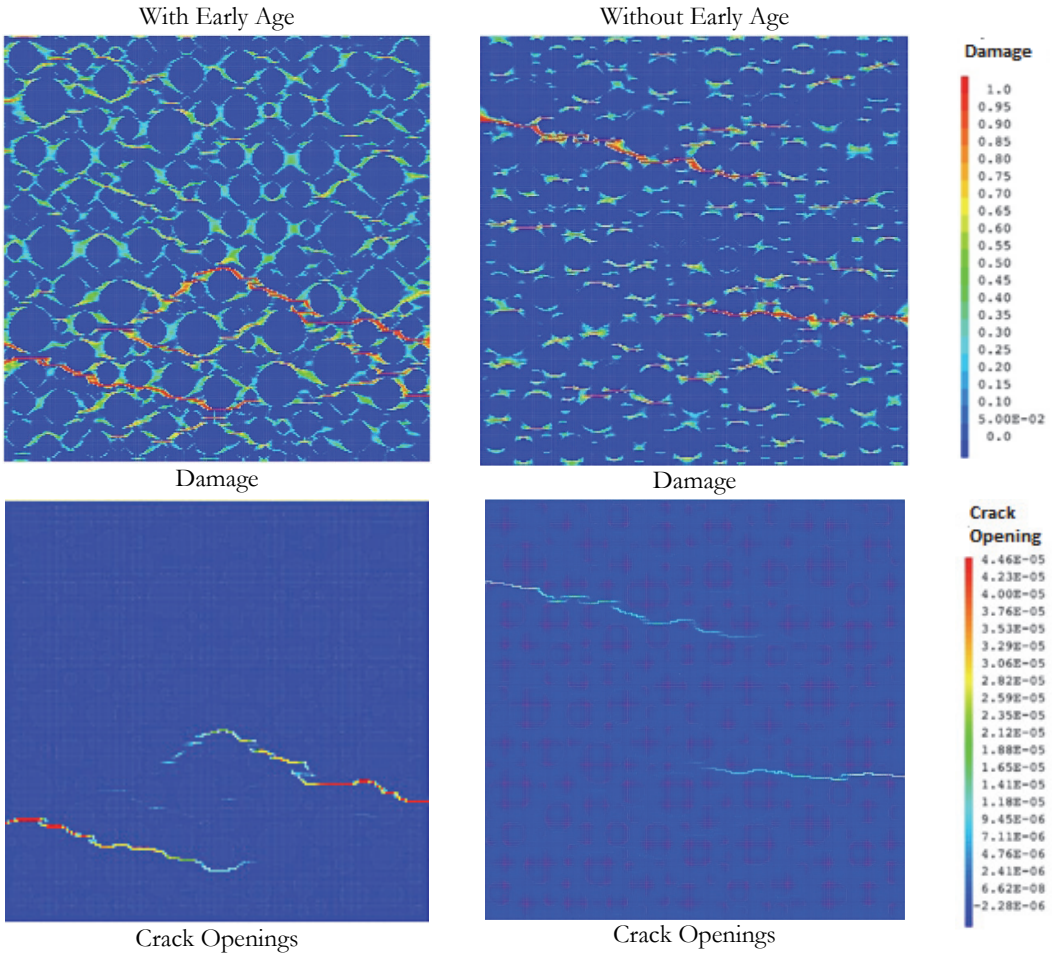

Figure 10: Damage and crack openings due to early age under traction

GLOBAL-LOCAL BEHAVIOUR UNDER CYCLIC LOADING.

There may be situations where additional or unpredicted loads may be encountered during the service life of concrete structures. During a seismic excitation and under cyclic loadings, crack opening-closing effects are observed. During a loading cycle, cracks open then close upon load reversal from tension to compression. During the load reversals, micro cracks close progressively and the tangent stiffness of the material should increase. In the damage model proposed above, the unilateral condition is taken into account by a separation of the stress tensor into positive and negative parts. In case of cyclic loadings, the stress is given:

$$\sigma = \langle \sigma \rangle_+ + \langle \sigma \rangle_- \tag{26}$$

$$\sigma_{ij} = (1-d^t)\left\langle C^0_{ijkl}\varepsilon_{kl}\right\rangle_+ + (1-d^c)\left\langle C^0_{ijkl}\left\langle C^0_{ijkl}\varepsilon_{kl}\right\rangle\right\rangle_- \tag{27}$$

The damage variables d^t and d^c describe the influence of damage on the response of the material in tension and compression respectively. The two variables are related by the following equations:

$$d^c = \left(d^t\right)^{\alpha} \tag{28}$$

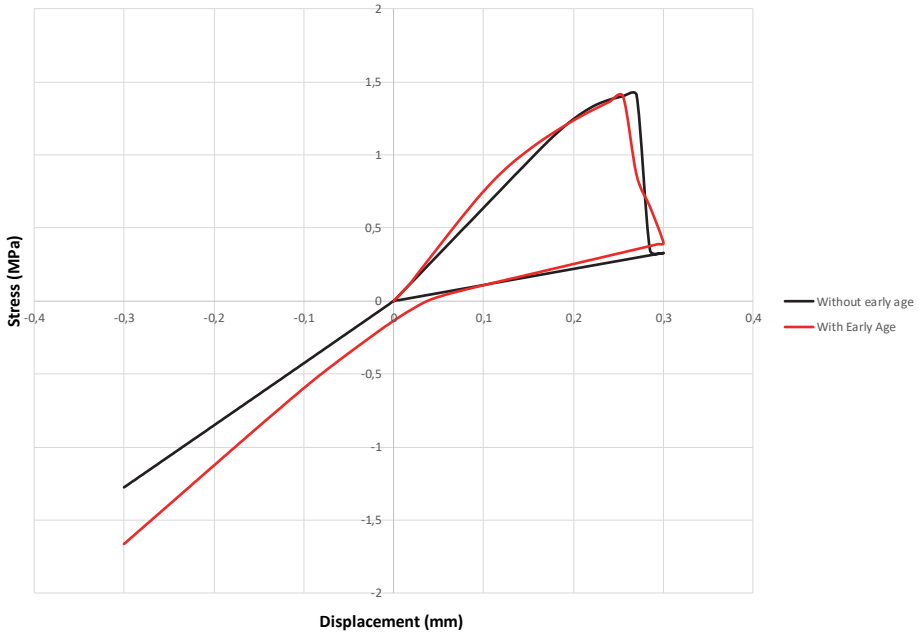

Figure 11: Global behaviour of concrete under cyclic loading.

As stated, concrete with early age exhibits a premature nonlinear behaviour due to the existence of initial stress state. Regarding the cyclic behaviour, as the closing process is driven by the stress tensor sign, the crack closure stress equal to $\sigma = 0$ correspond to a zero strain $\varepsilon = 0$ (Under tension, in Eqn. (27) $\varepsilon = 0 \Rightarrow \sigma = 0$). However, Fig. 11 depicts that the initial stress state (concrete with early age) due to the hydration process plays an important role. After complete unloading $\sigma = 0$, permanent displacements are observed. The reason being that the behaviour at early age computed is considered as an initial state (stresses, internal variables, displacements). This state of stress is at the origin of a part of the inelastic strains. Strictly speaking, for concrete with early age, complete unloading ($\sigma = 0$) does not correspond to zero deformations (displacements). Even if the model does not consider plastic strain, permanent displacements (corresponding to damage, inelastic strain, cracking) are observed. These irreversible strains are caused by the initial early age state.

Regarding the local behaviour, Fig. 12 shows the damage distribution and the crack opening values due after a loading cycle. After a complete unloading (ie $\sigma = 0MPa$), the maximum crack openings values obtained for concrete with early age is about $1.95\mu m$. For concrete without early age, cracks are closed (of about $0.04\mu m \approx 0$).

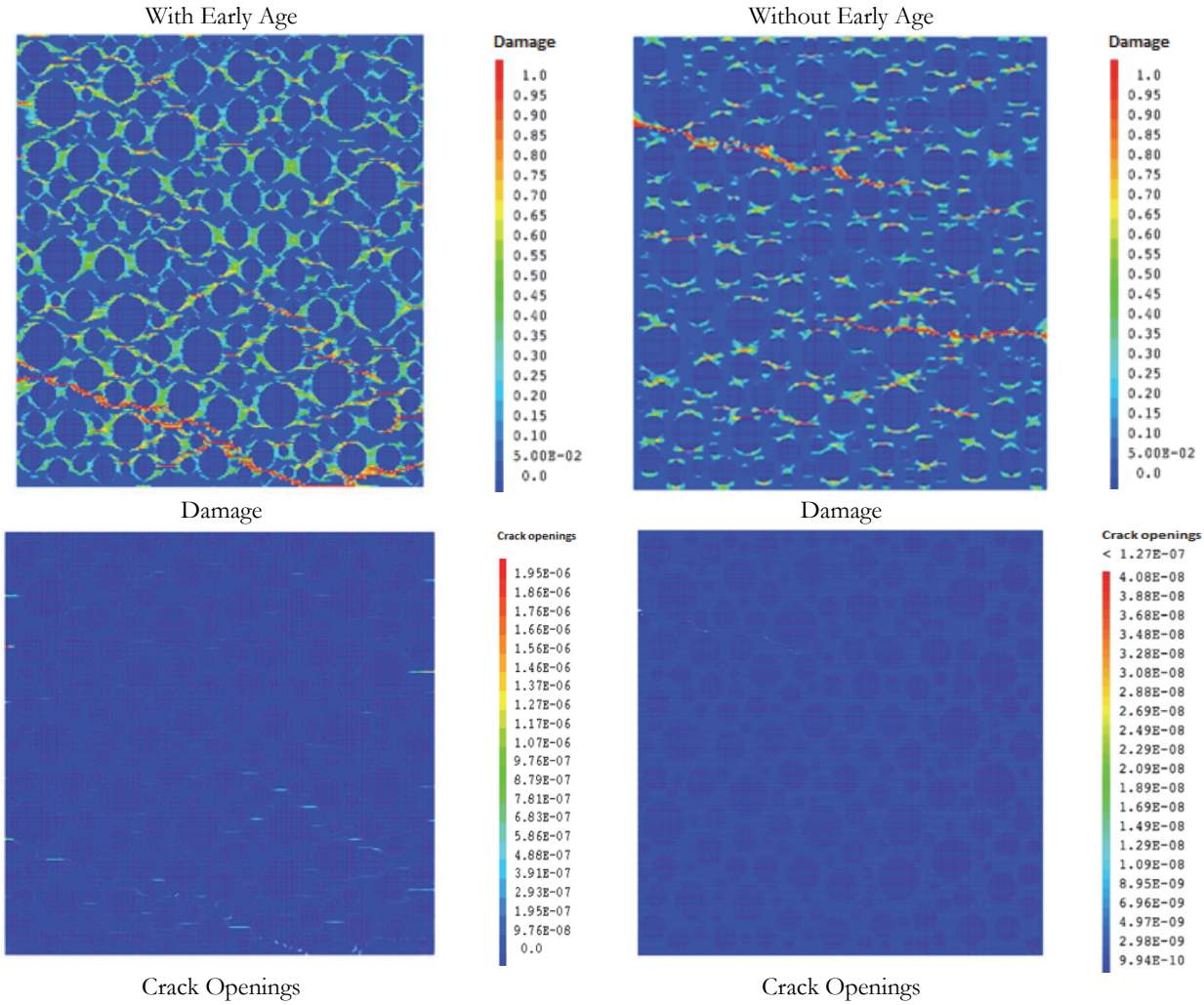

Figure 12: Damage and crack openings due to the early age after a loading cycle.

EFFECT OF AGGREGATE COOLING AND PIPE COOLING ON EARLY AGE CONCRETE

A study on the mass concrete hydration temperature control systems is undertaken with the resultant impact on the mechanical behaviour of concrete under tensile and cyclic loadings. The model parameters for the numerical computation of pipes and aggregate cooling systems were given in Tab. 4 and Tab. 5.

Fig. 13 shows the hydration temperature evolution of the two models. Aggregate cooling method has relatively lower initial and peak temperatures as compared to pipe cooling. The thermal evolution is almost comparable though better for pipes cooling system with relation to initial and final temperature fluctuations. Fig. 14 shows stress, damage and crack openings of aggregate and pipe cooled concrete samples due to early age hydration. The two systems permit to reduce the effect of the hydration process in terms of damage and cracks. The spatial distribution of damage is different. Aggregate cooling system gives a smeared distribution of damage. Lower values are obtained for both damage and crack openings for the two cooling systems compared to concrete without cooling.

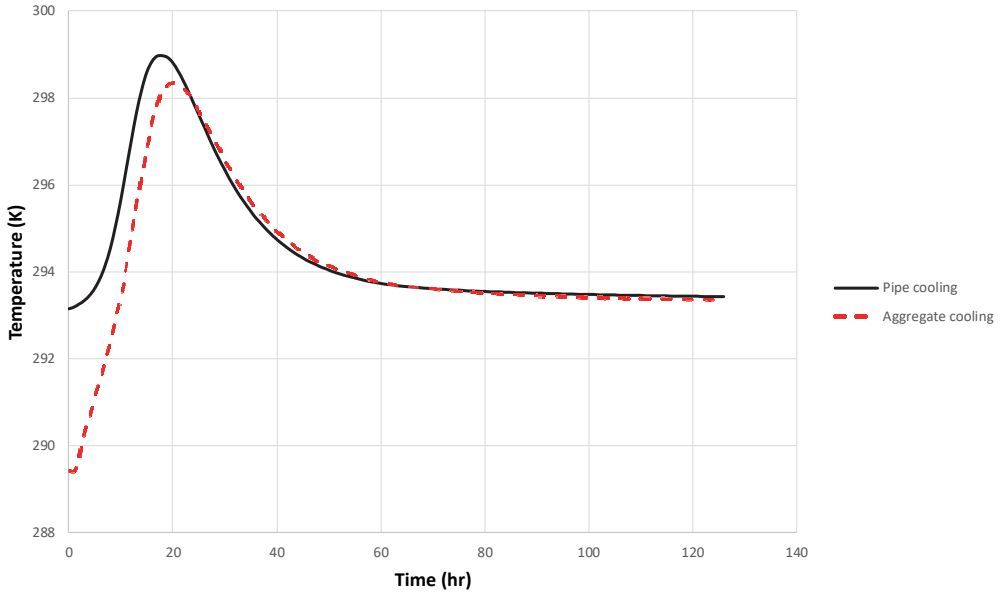

Figure 13: Hydration temperature evolution of an aggregate cooled model and a pipe cooled model.

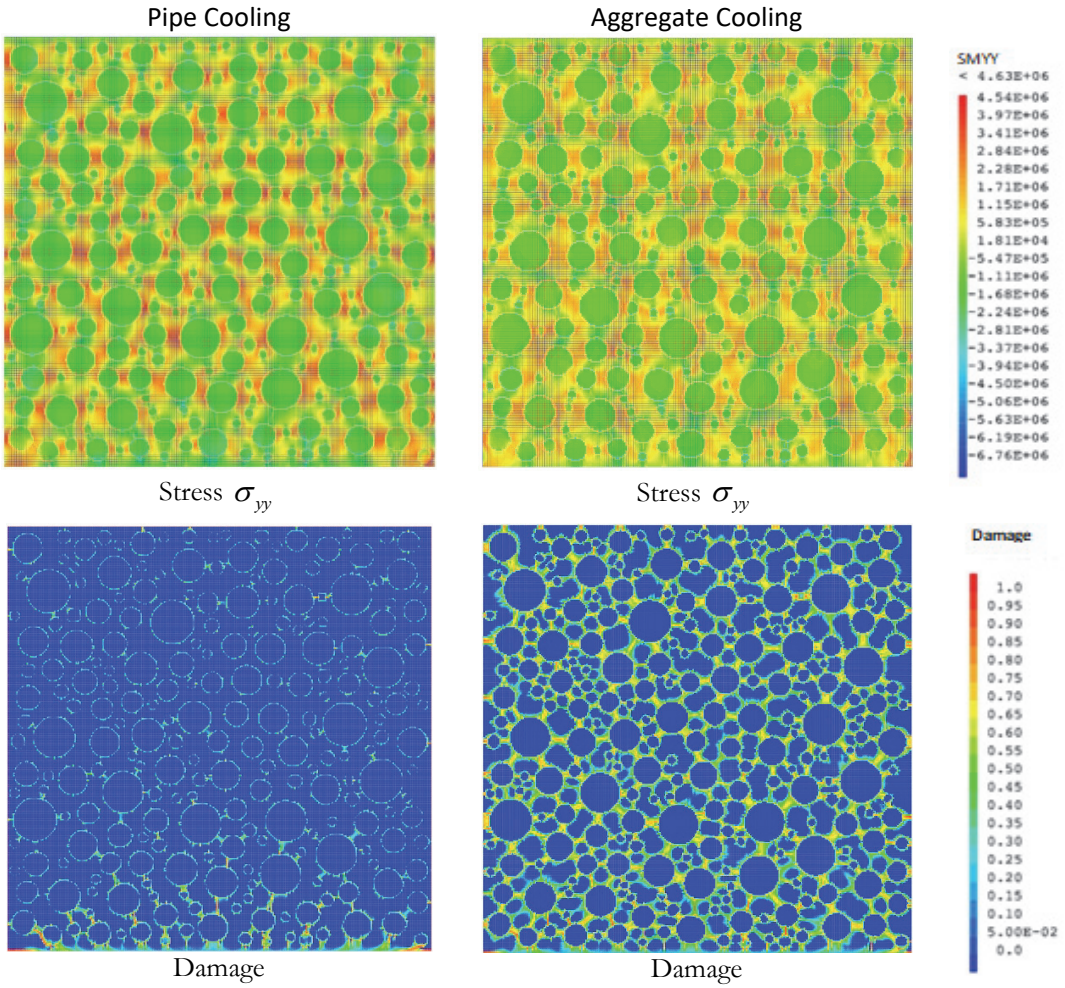

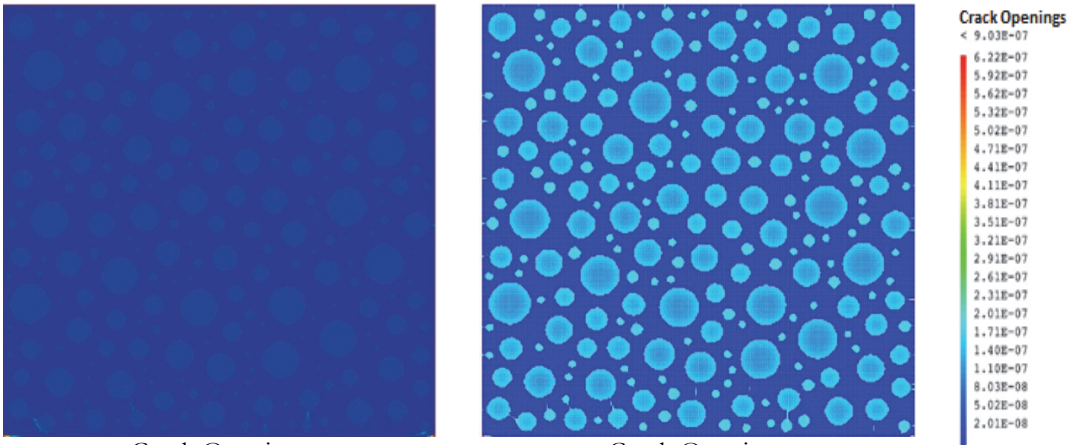

Figure 14: Stress, damage and crack openings due to early age (Aggregate and pipe cooled concrete).

EFFECT OF AGGREGATE COOLING AND PIPE COOLING ON EARLY AGE CONCRETE UNDER TENSILE LOADING

The impact of the hydration temperature control systems on the mechanical behaviour of concrete is investigated under tensile loadings. Fig. 15 shows the global behaviour of pipe and aggregate cooled early age concrete. Quite similar results are obtained regarding the peak stress. Both samples portray a brittle behaviour; however, the behaviour of pipe cooled concrete is more brittle. This result is in accordance with damage patterns obtained at early age. Smeared damage behaviour is obtained with aggregate cooling. As it has been outlined before, initial state due to early age leads to a premature non-linear behaviour. Fig. 16 shows that pipe and aggregate cooled concretes do not exhibit this behaviour; the elastic phase is characterized by a linear behaviour similar to concrete without early age. Overall, the result shows a significant improvement of concrete treated with these cooling methods.
Fig. 17 illustrates the evolution of damage and crack openings. Pipe cooled concrete exhibits a more localized damage and higher values of crack openings. This localisation is the consequence of the initial state computed at early age.

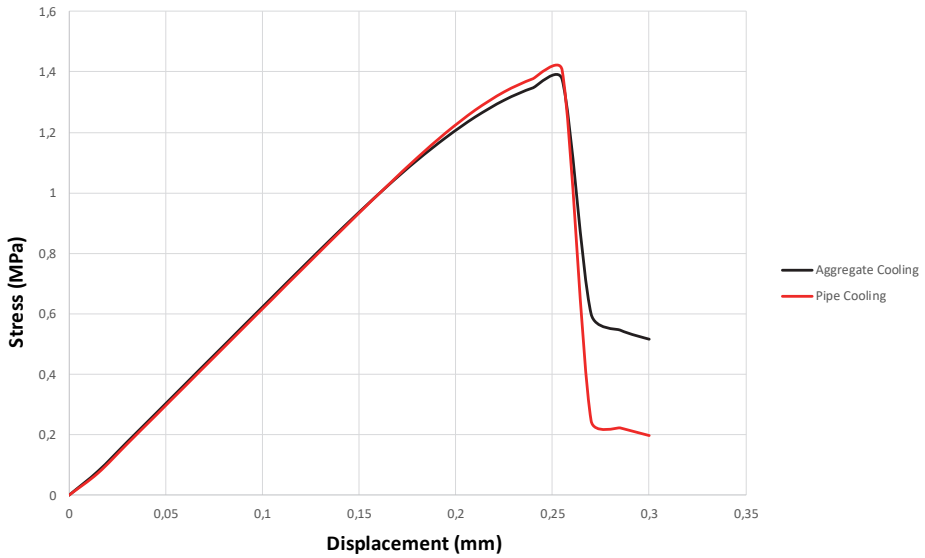

Figure 15: Global mechanical behaviour of pipe and aggregate cooled concrete samples under tension.

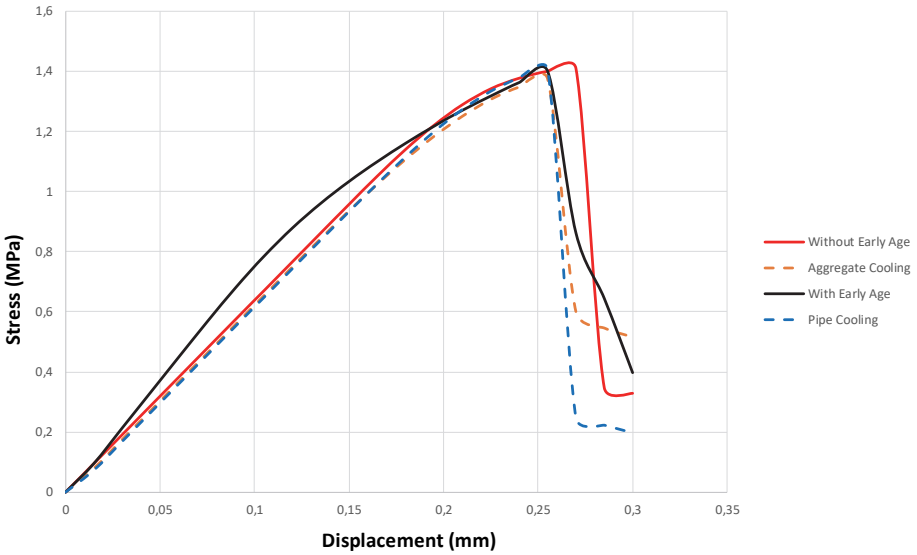

Figure 16: Global mechanical behaviour of aggregate, pipe cooled, early age (EA) concrete and concrete without early age (WEA) under tension.

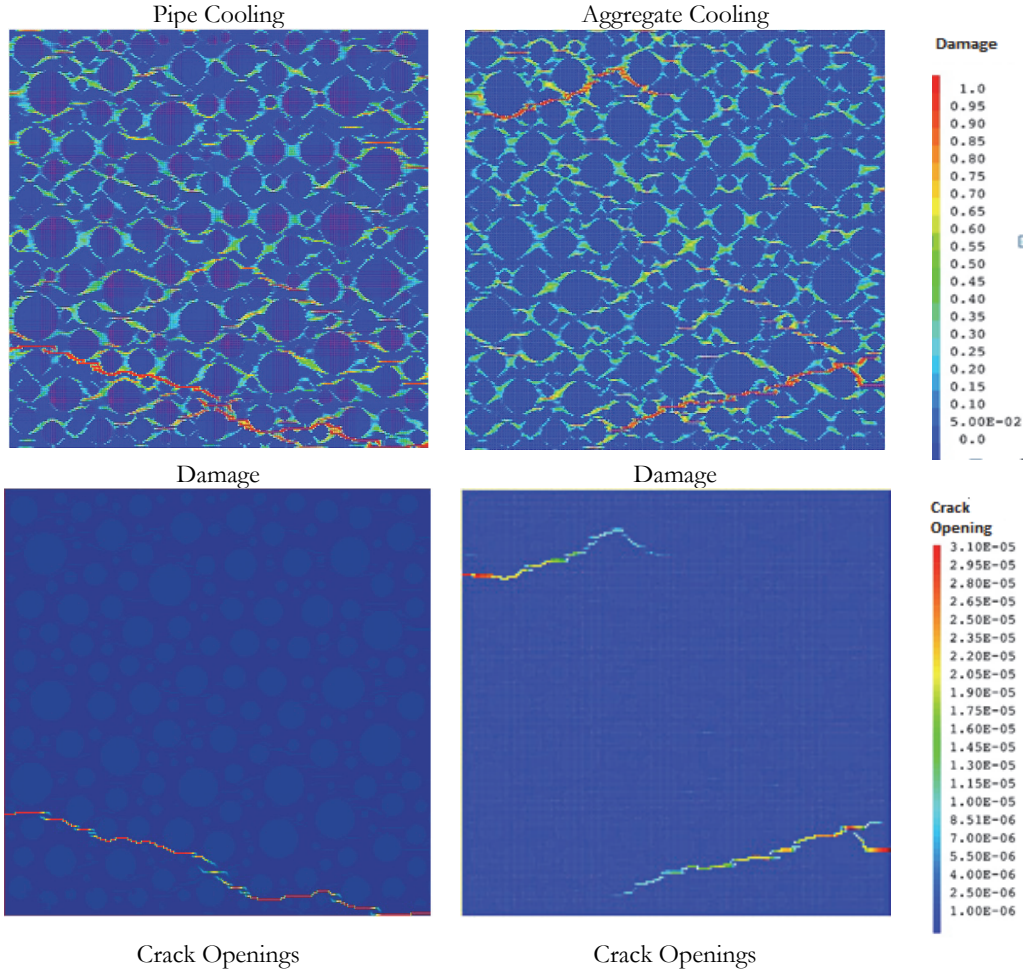

Figure 17: Damage and crack openings of concrete with early age under tension. (Aggregate and pipe cooled).

EFFECT OF AGGREGATE COOLING AND PIPE COOLING ON EARLY AGE CONCRETE UNDER CYCLIC LOADING

As it has been outlined before, when the specimen is subjected to a loading cycle (tension-compression cycle), due to the presence of the initial stress state, instead of obtaining zero displacements (as the model does not consider plastic strains), early age concrete exhibits permanent displacement at a complete unloading $\sigma = 0$. Fig. 18 shows that both pipe and aggregate cooling systems reduce the initial state resulting in lower permanent displacements compared to concrete without cooling. Fig. 19 shows a comparison of the global behaviour of different configurations (Early Age, Without Early Age, Pipe cooling, Aggregate cooling). Pipe and aggregate cooled concretes have similar behaviour to concrete without early age. Both controlling systems are efficient enough to reduce the effect of early age state.

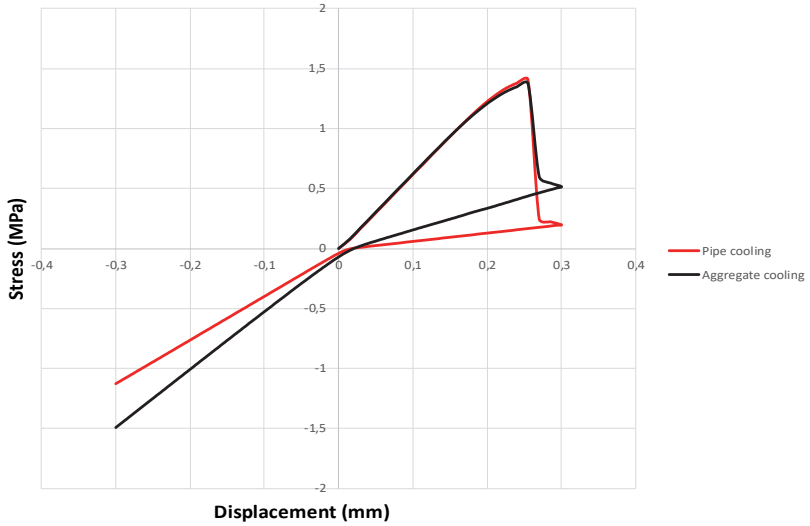

Figure 18: Global behaviour of concrete under cyclic loading (Aggregate and Pipe cooled).

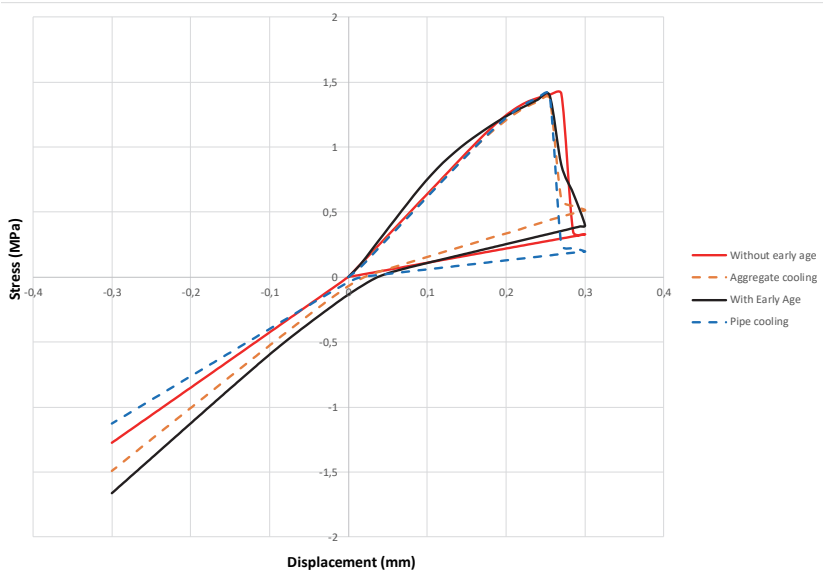

Figure 19: Global mechanical behaviour of aggregate, pipe cooled, EA concrete and WEA concrete under cyclic loading.

Fig. 20 shows the distribution of stresses, damage and crack openings of an aggregate and pipe cooled model under cyclic loading computed after a complete unloading $\sigma = 0$. Lower crack opening values are obtained compared to early age concrete. After complete recovering $\sigma = 0MPa$, the maximum crack openings values are 1.70 μm for aggregate cooled

concrete and 1.38 μm for pipe cooled concrete. These values are lower than those obtained for concrete at early age without cooling 1.95 μm (see Fig. 12).

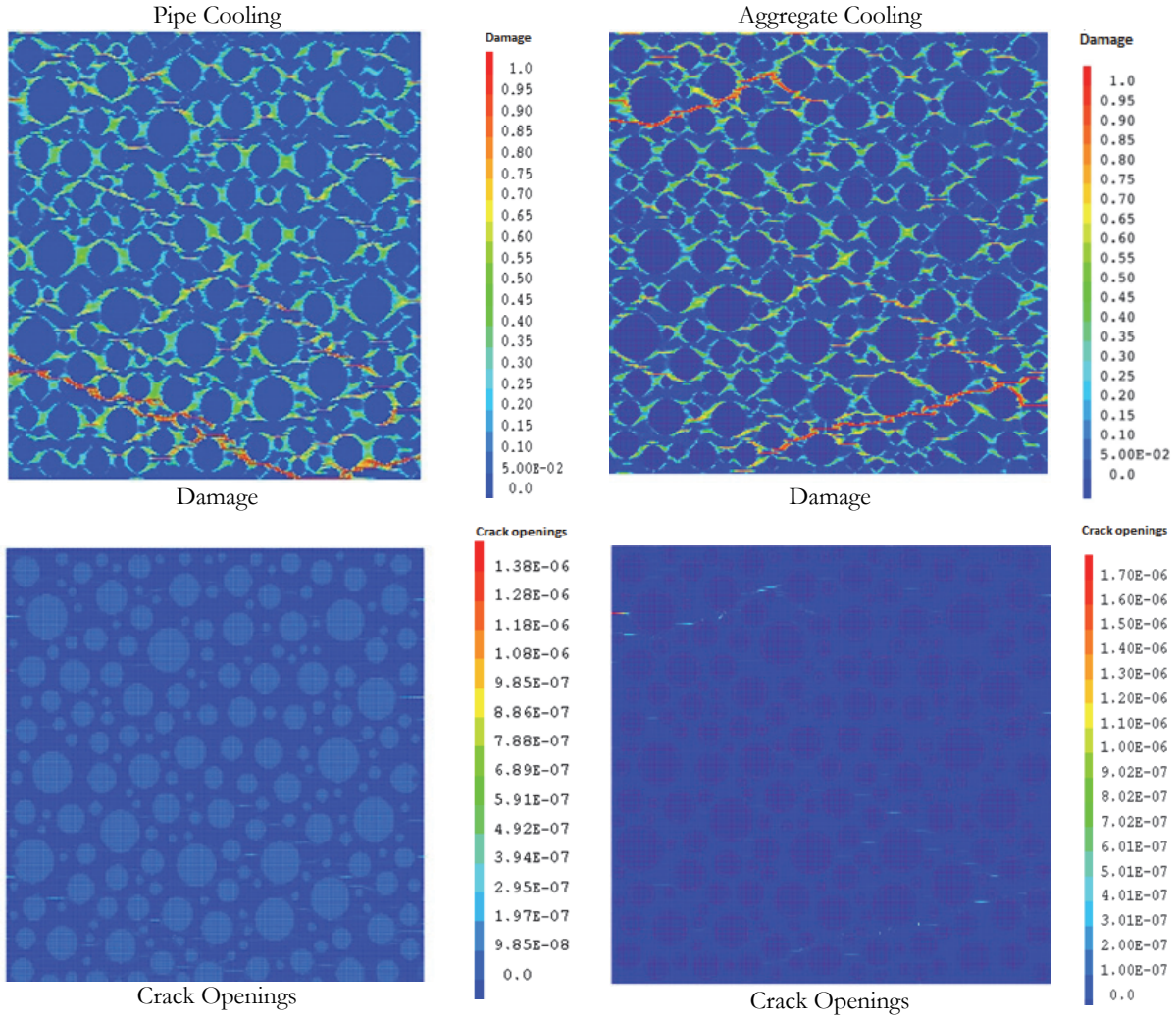

Figure 20: Damage and crack openings due to early age under cyclic loading. (Aggregate and pipe cooled).

CONCLUSION

A numerical investigation was carried out into the effect of pipe cooling and aggregate cooling methods on the mechanical behaviour of concrete. The numerical computations were driven using a Chemo-Thermo-Mechanical model. The early age behaviour has been investigated using the CTM model at a mesoscale level. The mechanical analysis of the consequences brought by this initial state has been investigated under tensile and cyclic loadings.

Observations show significant improvements regarding to final damage and cracking of concrete treated with cooling methods. Aggregate cooling method gives diffused damage with comparison to the pipe cooling method. Under tensile loading, the result shows a significant improvement of cooled concrete. Regarding the cyclic behaviour, initial state due to the hydration process leads to permanent displacements corresponding to damage and inelastic strains (cracking). Using pipe or aggregate cooled concrete can reduce the initial stress state and improve the behaviour of concrete during the service life of structures.

CONFLICTS OF INTEREST/COMPETING INTERESTS

The authors declare that they have no conflict of interest.

CODE AVAILABILITY

FEM software available at: http://www-cast3m.cea.fr/

AUTHORS' CONTRIBUTIONS

All the authors contributed to the design and implementation of the proposed approach, to the analysis of the results, and the writing of the manuscript.

REFERENCES

[1] Liu, J., Qin, W., Zhao, D., Dai, G. (2017). Investigating crack control in the mega-size concrete floors of an airport terminal, Int. J. Civ. Eng., 15(8), pp. 1203–1213, DOI: 10.1007/s40999-016-0135-x.
[2] Hernandez-Bautista, E., Bentz, D.P., Sandoval-Torres, S., Cano-Barrita, P.F. de J. (2016). Numerical simulation of heat and mass transport during hydration of Portland cement mortar in semi-adiabatic and steam curing conditions, Cem. Concr. Compos., 69, pp. 38–48, DOI: 10.1016/j.cemconcomp.2015.10.014.
[3] (2006). Evaluation of Temperature Prediction Methods for Mass Concrete Members, ACI Mater. J., 103(5), DOI: 10.14359/18158.
[4] Kjellsen, K.O., Detwiler, R.J., Gjørv, O.E. (1990). Pore structure of plain cement pastes hydrated at different temperatures, Cem. Concr. Res., 20(6), pp. 927–33, DOI: 10.1016/0008-8846(90)90055-3.
[5] Branco, F.A., Mendes, P., Mirambell, E. (1992). Heat of Hydration Effects in Concrete Structures, ACI Mater. J., 89(2), pp 139-145. DOI: 10.14359/2105.
[6] Ulm, F.-J., Coussy, O. (2001). What Is a "Massive" Concrete Structure at Early Ages? Some Dimensional Arguments, J. Eng. Mech., 127(5), pp. 512–522, DOI: 10.1061/(ASCE)0733-9399(2001)127:5(512).
[7] Shaikh, F.U.A. (2018). Effect of Cracking on Corrosion of Steel in Concrete, Int. J. Concr. Struct. Mater., 12(1), pp. 3, DOI: 10.1186/s40069-018-0234-y.
[8] ACI. (1998). ACI 207.4 R-93 - Cooling and Insulating Systems for Mass Concrete, Concrete, 93 (Reapproved), pp. 1–22.
[9] Juenger, M.C.G., Solt, S.M., Hema, J. (2010). Effects of Liquid Nitrogen Cooling on Fresh Concrete Properties, ACI Mater. J., 107(2), DOI: 10.14359/51663575.
[10] Su, H., Li, J., Wen, Z. (2014). Evaluation of Various Temperature Control Schemes for Crack Prevention in RCC Arch Dams During Construction, Arab. J. Sci. Eng., 39(5), pp. 3559–3569, DOI: 10.1007/s13369-014-1010-1.
[11] O'Leary, K.R.J. (2015). Cooling Concrete with Embedded Pipes, Concr. Int., 27(5).
[12] Singh, S.P., Murmu, M. (2017). Effects of Curing Temperature on Strength of Lime-Activated Slag Cement, Int. J. Civ. Eng., 15(4), pp. 575–584, DOI: 10.1007/s40999-017-0166-y.
[13] Bernardi, P., Cerioni, R., Michelini, E., Sirico, A. (2016). Numerical simulation of early-age shrinkage effects on RC member deflections and cracking development, Frat. Ed Integrità Strutt., 10(37), pp. 15–21, DOI: 10.3221/IGF-ESIS.37.03.
[14] Maruyama, I., Lura, P. (2019). Properties of early-age concrete relevant to cracking in massive concrete, Cem. Concr. Res., 123, pp. 105770, DOI: 10.1016/j.cemconres.2019.05.015.
[15] Zheng, Z., Wei, X. (2021). Mesoscopic models and numerical simulations of the temperature field and hydration degree in early-age concrete, Constr. Build. Mater., 266, pp. 121001, DOI: 10.1016/j.conbuildmat.2020.121001.
[16] Zhao, Y., Ding, D., Bi, J., Wang, C., Liu, P. (2021). Experimental study on mechanical properties of precast cracked concrete under different cooling methods, Constr. Build. Mater., 301, pp. 124141, DOI: 10.1016/j.conbuildmat.2021.124141.
[17] Liu, X., Zhang, C., Chang, X., Zhou, W., Cheng, Y., Duan, Y. (2015). Precise simulation analysis of the thermal field

in mass concrete with a pipe water cooling system, Appl. Therm. Eng., 78, pp. 449–459, DOI: 10.1016/j.applthermaleng.2014.12.050.
[18] ACI. (1980). Cooling and Insulating Systems for Mass Concrete., Concr. Int., 2(5), pp. 45–64.
[19] Fichant, S., La Borderie, C., Pijaudier-Cabot, G. (1999). Isotropic and anisotropic descriptions of damage in concrete structures, Mech. Cohesive-Frictional Mater., 4(4), pp. 339–359, DOI: 10.1002/(SICI)1099-1484(199907)4:4<339::AID-CFM65>3.0.CO;2-J.
[20] Guo, Y.B., Gao, G.F., Jing, L., Shim, V.P.W. (2017). Response of high-strength concrete to dynamic compressive loading, Int. J. Impact Eng., 108, pp. 114–135, DOI: 10.1016/j.ijimpeng.2017.04.015.
[21] Le Minh, H.-., Khatir, S., Abdel Wahab, M., Cuong-Le, T. (2021). A concrete damage plasticity model for predicting the effects of compressive high-strength concrete under static and dynamic loads, J. Build. Eng., 44, pp. 103239, DOI: 10.1016/j.jobe.2021.103239.
[22] Le Thanh, C., Minh, H.-L., Sang-To, T. (2021). A nonlinear concrete damaged plasticity model for simulation reinforced concrete structures using ABAQUS, Frat. Ed Integrità Strutt., 16(59), pp. 232–242, DOI: 10.3221/IGF-ESIS.59.17.
[23] Ulm, F.-J., Coussy, O. (1995). Modeling of Thermochemomechanical Couplings of Concrete at Early Ages, J. Eng. Mech., 121(7), pp. 785–794, DOI: 10.1061/(ASCE)0733-9399(1995)121:7(785).
[24] Briffaut, M., Benboudjema, F., Torrenti, J.M., Nahas, G. (2011). A thermal active restrained shrinkage ring test to study the early age concrete behaviour of massive structures, Cem. Concr. Res., 41(1), pp. 56–63, DOI: 10.1016/j.cemconres.2010.09.006.
[25] Matallah, M., La Borderie, C., Maurel, O. (2009). A practical method to estimate crack openings in concrete structures, Int. J. Numer. Anal. Methods Geomech, DOI: 10.1002/nag.876.
[26] De Borst, R., Sluys, L.J., Muhlhaus, H. -B., Pamin, J. (1993). Fundamental issues in finite element analyses of localization of deformation, Eng. Comput., 10(2), pp. 99–121, DOI: 10.1108/eb023897.
[27] Pascuzzo, A., Greco, F., Leonetti, L., Lonetti, P., Pranno, A., Ronchei, C. (2022). Investigation of mesh dependency issues in the simulation of crack propagation in quasi-brittle materials by using a diffuse interface modeling approach, Fatigue Fract. Eng. Mater. Struct., 45(3), pp. 801–820, DOI: 10.1111/ffe.13635.
[28] Bažant, Z.P., Oh, B.H. (1983). Crack band theory for fracture of concrete, Matériaux Constr., 16(3), pp. 155–177, DOI: 10.1007/BF02486267.
[29] Matallah, M., Aissaoui, N. (2020). Mesomechanical Investigation of the Relationship between the Length of the Fracture Process Zone and Crack Extensions in Concrete, Phys. Mesomech., 23(6), pp. 494–508, DOI: 10.1134/S1029959920060053.
[30] Aissaoui, N., Matallah, M. (2017). Numerical and analytical investigation of the size-dependency of the FPZ length in concrete, Int. J. Fract., 205(2), pp. 127–138, DOI: 10.1007/s10704-017-0186-2.
[31] Matallah, M., La Borderie, C. (2016).3D Numerical Modeling of the Crack-Permeability Interaction in Fractured Concrete. Proceedings of the 9th International Conference on Fracture Mechanics of Concrete and Concrete Structures, IA-FraMCoS.
[32] Neville, M., Dilger, W. H. (1983). Creep of plain and structural concrete, London.
[33] De Schutter, G., Taerwe, L. (1996). Degree of hydration-based description of mechanical properties of early age concrete, Mater. Struct., 29(6), pp. 335–344, DOI: 10.1007/BF02486341.
[34] Matallah, M., Farah, M., Grondin, F., Loukili, A., Rozière, E. (2013). Size-independent fracture energy of concrete at very early ages by inverse analysis, Eng. Fract. Mech., 109, pp. 1–16, DOI: 10.1016/j.engfracmech.2013.05.016.
[35] Sofi, M., Mendis, P., Baweja, D., Mak, S. (2014). Influence of ambient temperature on early age concrete behaviour of anchorage zones, Constr. Build. Mater., 53, pp. 1–12, DOI: 10.1016/j.conbuildmat.2013.11.051.
[36] Nguyen, D., Lawrence, C., La Borderie, C., Matallah, M., Nahas, G. (2010). A mesoscopic model for a better understanding of the transition from diffuse damage to localized damage, Eur. J. Environ. Civ. Eng., 14(6–7), pp. 751–76, DOI: 10.1080/19648189.2010.9693261.
[37] Grondin, F., Matallah, M. (2014). How to consider the Interfacial Transition Zones in the finite element modelling of concrete?, Cem. Concr. Res., 58, pp. 67–75, DOI: 10.1016/j.cemconres.2014.01.009.
[38] Cast3M, 'Finite element code,' [Online]. Available: http://www-cast3m.cea.fr/.
[39] Nguyen, T.-C., Huynh, T.-P., Tang, V.-L. (2019). Prevention of crack formation in massive concrete at an early age by cooling pipe system, Asian J. Civ. Eng., 20(8), pp. 1101–1107, DOI: 10.1007/s42107-019-00175-5.